THE JOURNAL OF BIOLOGICAL CHEMISTRY
Vol. 279, No. 17, Issue of April 23, pp. 17260–17268, 2004

Printed in U.S.A.

$G\alpha_{i1}$ and $G\alpha_{i3}$ Differentially Interact with, and Regulate, the G Protein-activated K^+ Channel*

Received for publication, December 9, 2003, and in revised form, February 3, 2004
Published, JBC Papers in Press, February 12, 2004, DOI 10.1074/jbc.M313425200

Tatiana Ivanina‡, Dalia Varon‡, Sagit Peleg‡, Ida Rishal‡, Yuri Porozov‡, Carmen W. Dessauer§, Tal Keren-Raifman‡, and Nathan Dascal‡¶

From the ‡Department of Physiology and Pharmacology, Sackler School of Medicine, Tel Aviv University, Ramat Aviv 69978, Israel and the §Department of Integrative Biology and Pharmacology, University of Texas-Houston Medical School, Houston, Texas 77030

G protein-activated K^+ channels (GIRKs; Kir3) are activated by direct binding of $G\beta\gamma$ subunits released from heterotrimeric G proteins. In native tissues, only pertussis toxin-sensitive G proteins of the $G_{i/o}$ family, preferably $G\alpha_{i3}$ and $G\alpha_{i2}$, are donors of $G\beta\gamma$ for GIRK. How this specificity is achieved is not known. Here, using a pull-down method, we confirmed the presence of $G\alpha_{i3\text{-}GDP}$ binding site in the N terminus of GIRK1 and identified novel binding sites in the N terminus of GIRK2 and in the C termini of GIRK1 and GIRK2. The non-hydrolyzable GTP analog, guanosine 5′-3-*O*-(thio)triphosphate, reduced the binding of $G\alpha_{i3}$ by a factor of 2–4. $G\alpha_{i1\text{-}GDP}$ bound to GIRK1 and GIRK2 much weaker than $G\alpha_{i3\text{-}GDP}$. Titrated expression of components of signaling pathway in *Xenopus* oocytes and their activation by m2 muscarinic receptors revealed that G_{i3} activates GIRK more efficiently than G_{i1}, as indicated by larger and faster agonist-evoked currents. Activation of GIRK by purified $G\beta\gamma$ in excised membrane patches was strongly augmented by coexpression of $G\alpha_{i3}$ and less by $G\alpha_{i1}$. Differences in physical interactions of GIRK with GDP-bound $G\alpha$ subunits, or $G\alpha\beta\gamma$ heterotrimers, may dictate different extents of $G\alpha\beta\gamma$ anchoring, influence the efficiency of GIRK activation by $G\beta\gamma$, and play a role in determining signaling specificity.

The importance of G protein-activated K^+ channels (GIRK; Kir3)[1] is 2-fold: as abundant mediators of inhibitory neuronal signaling and as the first known and one of the best studied direct effectors of $G\beta\gamma$ (1, 2). GIRK channels convey inhibitory signals of many neurotransmitters acting via G protein-coupled receptors (GPCRs). They mediate much of the negative inotropic effect of acetylcholine (ACh) acting via the m2 muscarinic receptor (m2R) in the heart (3, 4) and many of the inhibitory actions of opioids, serotonin, γ-aminobutyric acid, dopamine, and other transmitters in the brain (2, 5). They also play important roles in neuronal regulations of behavior and in mediation of GPCR- and alcohol-induced analgesia (6, 7). GIRKs are inwardly rectifying, tetrameric K^+ channels. GIRK1/2 heterotetramers, abundant in the brain, and GIRK1/4, prevailing in the heart, display a $GIRK1_2GIRKx_2$ stoichiometry. Each subunit consists of a core transmembrane domain with two membrane-spanning α-helixes M1 and M2, flanked by cytoplasmic N and C termini, and a re-entrant helix-P-loop between M1 and M2. Recently resolved crystal structures of the cytoplasmic domain of GIRK1 and of an entire bacterial inward rectifier KirBac1.1 (8, 9) show that the cytosolic domains of Kir channels tetramerize to form a cytoplasmic water-filled channel that presents continuation of the transmembrane pore (see Fig. 1*A*).

It is now unequivocally established that $G\beta\gamma$, but not $G\alpha$, activates GIRK (10). $G\beta\gamma$ binds to sites located in the N and C termini of each GIRK subunit and triggers channel opening by an unknown mechanism (11). The role of $G\alpha$ subunits in GIRK signaling has been controversial for many years (reviewed in Ref. 10), but it is now becoming clear that $G\alpha$ subunits are not mere donors of $G\beta\gamma$ for GIRK activation. They physically interact with GIRK, and it has been proposed that they contribute to channel function in several ways: determining the specificity of activation by neurotransmitters, anchoring the $G\beta\gamma$ subunits to GIRK to ensure fast and specific activation (12, 13), and regulating GIRK basal activity and $G\beta\gamma$-dependent gating (14). The latter seems to involve $G\alpha_{GDP}$ rather than $G\alpha_{GTP}$. In *Xenopus* oocytes, expression of $G\alpha_{i3}$ reduces an excessively high basal activity of overexpressed GIRK channels and enhances agonist-induced activation. In excised patches, coexpressed $G\alpha_{i3}$ enhanced GIRK activation caused by added $G\beta\gamma$ protein. This suggested that $G\alpha_{i3}$ (probably in its GDP-bound form) not only sequesters free $G\beta\gamma$ and donates it upon agonist activation, but also predisposes (primes) the channels to $G\beta\gamma$ activation (14). It is not known whether the priming effect is also produced by $G\alpha$ subunits other than $G\alpha_{i3}$.

The role of $G\alpha$ in the specificity of signaling from GPCR to GIRK is widely accepted (15), but the mechanisms are unclear. GIRK is similarly activated by all $G\beta\gamma$ tested (16, 17) except $G\beta_5$ which, in combination with $G\gamma_2$, inhibits GIRK (17). However, in native tissues, $G\beta_5$ is associated mainly with certain RGS (regulators of G protein signaling) proteins rather than $G\gamma$ (18, 19). Therefore, it is unlikely that selectivity of coupling is determined by $G\beta\gamma$; $G\alpha$ subunits must play a role. In cardiac and neuronal cells only pertussis toxin-sensitive G proteins, $G\alpha_{i/o}$, activate GIRK (10). Selectivity is observed even within the $G_{i/o}$ family: in atrial and certain neuroendocrine and neuronal cells, upon activation of a variety of GPCRs, $G\alpha_{i2}$ and $G\alpha_{i3}$ rather than $G\alpha_{i1}$ and $G\alpha_o$ appear to be the preferred donors of $G\beta\gamma$ for GIRK (see "Discussion"). The molecular mechanisms determining the specific activation of GIRK only by certain G proteins remain unknown.

* This work was supported by National Institutes of Health Grants GM60419 (to C. D.) and GM68493 (to N. D.) and by the USA-Israel Binational Science Foundation (to N. D. and C. D.). The costs of publication of this article were defrayed in part by the payment of page charges. This article must therefore be hereby marked "*advertisement*" in accordance with 18 U.S.C. Section 1734 solely to indicate this fact.

¶ To whom correspondence should be addressed: Tel.: 972-3-640-5743; Fax: 972-3-640-9113; E-mail: dascaln@post.tau.ac.il.

[1] The abbreviations used are: GIRK, G protein-activated K^+ channel; aa, amino acid(s); GST, glutathione *S*-transferase; GPCR, G protein-coupled receptor; m2R, muscarinic receptor type 2; GTPγS, guanosine 5′-3-*O*-(thio)triphosphate; CHAPS, 3-[(3-cholamidopropyl)dimethylammonio]-1-propanesulfonic acid; c.a., cell-attached; ACh, acetylcholine.

In contrast to the normal physiological situation, in heterologous expression systems (*Xenopus* oocytes, Chinese hamster ovary and human embryonic kidney cells) GIRK can be activated by $G\beta\gamma$ released from a variety of G protein heterotrimers. Any $G\alpha_{i/o}$ (14, 20, 21), including the pertussis toxin-insensitive $G\alpha_z$, activates GIRK (22, 23). Even $G\alpha_s$ can donate $G\beta\gamma$ to activate GIRK in heterologous expression systems or in native cardiomyocytes if various components of the signaling pathway (β-adrenergic receptors, $G\alpha_s$, or $G\beta\gamma$) are overexpressed (24–26). Of all $G\alpha$ tested, only $G\alpha_q$ is unable to donate $G\beta\gamma$ in expression systems; activation of G_q by the relevant GPCRs inhibits GIRK, apparently via indirect pathways that involve second messengers (27, 28).

How, then, is the selective activation of GIRK via $G_{i/o}$ in native cardiac and neuronal cells ensured? Evidently, selective coupling between GPCRs and $G\alpha\beta\gamma$ heterotrimers contributes to the specificity of signaling to GIRK by neurotransmitters (20, 29), but this cannot explain the selectivity at the G protein-GIRK interface (*e.g.* why G_q does not activate GIRK). Thus, factors such as colocalization or scaffolding may be involved in assigning the relevant $G\alpha$ to GIRK. It has been proposed that pre-formed complexes of GIRK with certain $G\alpha\beta\gamma$ heterotrimers may exist in native cells, assuring fast and selective activation of GIRK by $G\beta\gamma$ derived from the GIRK-anchored heterotrimer (12, 13, 30). Supportive evidence is that $G\alpha_{i1}$ and $G\alpha_{i3}$ bind to the N terminus and mutations in N terminus reduce the speed of activation of GIRK by agonists of GIRK1 (12, 14, 31). However, this attractive hypothesis has not been conclusively confirmed.

Fundamental questions regarding the proposed complexes of GIRK with regulatory proteins remain open: whether GIRK subunits besides GIRK1 bind $G\alpha_i$; whether additional $G\alpha$-binding segments besides N terminus exist in GIRK; whether other $G\alpha$ subunits besides $G\alpha_{i1}$ and $G\alpha_{i3}$ bind to GIRK; and whether differences in binding of various $G\alpha$ subunits to GIRK contribute to signaling specificity and gating. To start to address these problems, we compared $G\alpha_{i3}$ and $G\alpha_{i1}$ subunits, which showed striking differences in their binding to GIRK in a preliminary comparative assay, for their ability to directly interact with the channel molecule and for their ability to regulate the physiological parameters of channel function. We identified and mapped $G\alpha_{i3}$ binding sites in N- and C-terminal parts of GIRK1 and GIRK2 subunits and then performed a comparative study of binding and physiological effects of $G\alpha_{i3}$ and $G\alpha_{i1}$. We found that $G\alpha_{i3}$ was a much better binding partner for GIRK1 and GIRK2 (at all binding sites) and a better physiological companion for $G\beta\gamma$ in GIRK activation. The correlation between binding and function of these two $G\alpha$ subunits supports a role for physical interaction between $G\alpha_{GDP}$ and GIRK in determining selective regulation of GIRK by different $G\alpha$ subunits.

EXPERIMENTAL PROCEDURES

Maintenance and operation of *Xenopus laevis* frogs, preparation and injection of RNA, and two-electrode voltage and patch clamp procedures have been performed as described previously (14, 27). Briefly, oocytes were incubated at 20–22 °C in ND96 solution (96 mM NaCl, 2 mM KCl, 1 mM $MgCl_2$, 1 mM $CaCl_2$, 5 mM HEPES, pH 7.5), supplemented with 2.5 mM sodium pyruvate and 50 μg/ml gentamicin. Data acquisition and analysis were done using the Axotape and the pCLAMP software (Axon Instruments). All experiments were done at 20–22 °C. Whole cell GIRK currents were measured using two-electrode voltage clamp at −80 mV in a high K^+ solution containing 24 mM KCl, 72 mM NaCl, 1 mM $CaCl_2$, 1 mM $MgCl_2$, 5 mM Hepes (pH 7.5). In patch clamp experiments, currents were recorded at −80 mV, filtered at 2 kHz, and sampled at 5 kHz. Pipette solution contained, in mM: 144 KCl, 2 NaCl, 1 $MgCl_2$, 1 $CaCl_2$, 1 $GdCl_3$, 10 Hepes/KOH, pH 7.5. Bath solution contained, in millimolar: 130 KCl, 2 $MgCl_2$, 1 EGTA, 2 Mg-ATP, 10 Hepes/KOH, pH 7.5. Stock solution of the purified recombinant $G\beta\gamma$ (40 μM) was diluted into 50 μl of the bath solution, added to the 500-μl solution in the bath, and stirred.

The cDNAs, mRNAs, GST fusion proteins, and total oocyte membrane fraction were prepared as described in our previous publications (14, 32), with minor modifications. Two buffers were used in pull-down experiments: phosphate-buffered saline or a 150 mM-K^+ buffer (in mM: 50 Tris, 5 $MgCl_2$, 1 EDTA, 150 KCl, pH 7.5). Identical binding patterns were seen in both buffers. [^{35}S]Methionine-labeled $G\alpha$ proteins were synthesized in reticulocyte lysate for 1.5–2 h, then 2–5 μl of lysate were incubated with 100 μM of either GDP or GTPγS for 30 min at 30 °C in 50 or 95 μl of binding buffer with the detergent of choice, 0.05% Tween 20 or 0.5% CHAPS. To measure $G\alpha$ binding to GST fusion proteins, 5–10 μg of the GST fusion protein were added, the total reaction volume brought to 300 or 500 μl, and the incubation continued in the presence of 100 μM GTPγS or GDP for 1–2 h at room temperature, and binding to glutathione-Sepharose beads and elution with 15 mM glutathione were done as described previously (14). The eluted proteins were run on 10% or 12% polyacrylamide-SDS gels (SDS-PAGE). The radioactive signals from protein bands of the gels were imaged and quantitated using PhosphorImager and the software ImageQuaNT (Molecular Dynamics). The readings were corrected for the differences in the amounts of GST fusion proteins eluted from the beads as measured from Coomassie Blue-stained gels (in most cases such differences did not exceed 50%). The full-length N terminus of GIRK1, $G1_{1-84}$, bound $G\alpha_{i3}$ as well as its distal part, $G1_{34-86}$ (data not shown), and the results obtained with these two proteins were pooled. For trypsin digestion, 1 μl of 0.25% stock of trypsin was diluted ×100 and incubated for 20 min at 30 °C with 30 μl of 150 mM-K^+ buffer with 0.5% CHAPS containing 2 μl of $G\alpha$ lysate, treated with GTPγS or GDP as described above. Western blots were done using standard procedures, using a common $G\alpha_i$ antibody (Calbiochem) and ECL reagents from Pierce Inc. Intensity of Coomassie Blue labeling was quantified using TINA software (Raytest, Straubenhardt, Germany).

Results are shown as mean ± S.E.; numbers of cells, patches, or separate biochemical determinations are shown *above the bars* in the figures. Multiple group comparison was done using one-way analysis of variance followed by Student-Newman-Keuls or Tukey's tests. *One* or *two asterisks* indicate $p < 0.05$ and $p < 0.01$, respectively, compared with control group. Values of $t_{90\%}$ parameters in $G\alpha_{i1}$- and $G\alpha_{i3}$-expressing groups, which report measurements independent of the control group, were compared by *t* test.

RESULTS

We explored the binding of $G\alpha_{i3}$ to GST-fused fragments of cytoplasmic N and C termini of GIRK1, using a standard pull-down method (Fig. 1*B*). The GST fusion proteins were immobilized of glutathione-agarose affinity beads. [^{35}S]Methionine-labeled $G\alpha_{i3}$ was synthesized *in vitro* in rabbit reticulocyte lysate, as it was done previously to study the interaction of $G\alpha_{i3}$ with the N terminus of GIRK1 (14). *In vitro* synthesized $G\beta\gamma$ has also been successfully utilized to identify $G\beta\gamma$ binding sites of voltage-gated Ca^{2+} and GIRK channels (32, 33). The binding experiments were routinely conducted in buffers containing 0.5% CHAPS, which minimized nonspecific binding of $G\alpha_{i3}$ to GST. All initial screening and mapping experiments reported in Figs. 1 and 2 were performed with GDP-bound $G\alpha_{i3}$ (see "Experimental Procedures"). In each experiment the amount of bound $G\alpha$ protein was measured from autoradiograms using a PhosphorImager and normalized to the amount of the bound G1–C3 segment, which was present in all experiments (Fig. 1*C*). We stress that this methodology gives a highly sensitive and accurate quantitation of bound protein, because the radioactive signal from labeled $G\alpha$ is measured from dried gels by using the PhosphorImager directly, in an almost unlimited linear range, and with high precision. In comparison, in Western blotting, several additional intermediate steps are involved, which reduce the accuracy of measurement.

In initial experiments, we found that not only the N terminus of GIRK1, but also the full-length C terminus of GIRK1 ($G1_{183-501}$) and of GIRK2 bound $G\alpha_{i3}$ (Fig. 1*C* and data not shown). We then examined the binding of $G\alpha_{i3\text{-}GDP}$ to the whole C terminus and to six non-overlapping GST-fused fragments of C terminus, G1–C1 through G1–C6 (Fig. 1*B*), previously used to map the

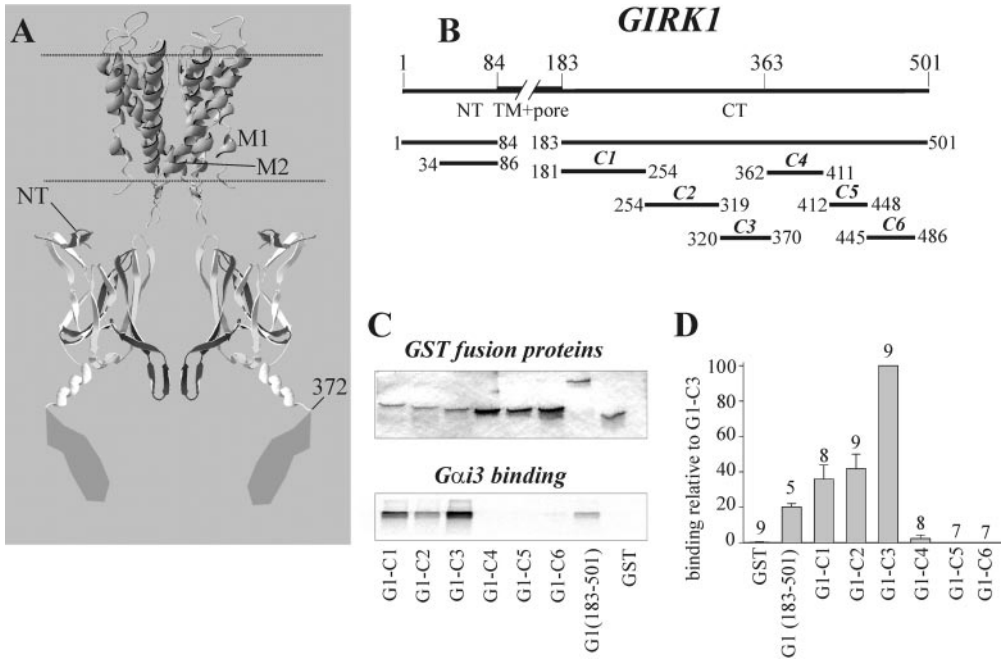

FIG. 1. **GST-fused fragments of GIRK1 bind Gα$_{i3\text{-}GDP}$.** *A*, schematic presentation of a GIRK channel. The image was made using the program Swiss PDB Viewer. The transmembrane part is shown as for KcsA (60). The *dashed lines* represent the approximate boundaries of the lipid phase of the membrane. Cytosolic domains of two out of four subunits are shown according to Nishida and MacKinnon (8). The folding of the C terminus of GIRK1 between residues 372 and 501 is not known and is shown arbitrarily. Linkers between cytoplasmic and transmembrane parts have not been resolved in the crystal structure of GIRK. Parts of the C terminus of GIRK1 tinted *black*, *gray*, and *light gray* correspond to G1–C1, G1–C2, and G1–C3, respectively. *B*, linear presentation of GIRK is shown at the *top*, and the GST-fused segments, with numbers of first and last amino acids, are shown *below*. *NT*, N terminus; *CT*, C terminus; *TM*, transmembrane domain. *C*, a representative pull-down experiment showing the binding of Gα$_{i3\text{-}GDP}$ to GST fusion proteins of GIRK1. The *upper panel* shows Coomassie Blue-stained proteins eluted from the beads and subjected to SDS-PAGE, and the *lower panel* shows a PhosphorImager autoradiogram of the bound [^{35}S]methionine-labeled Gα$_{i3}$. Note that the Gα-binding GST fusion proteins in this experiment (G1–C1 through G1–C3, and G1$_{183–501}$) have been added in lower amounts than GST fusion proteins of the second half of C terminus (G1–C4 through G1–C6); despite this, the latter did not bind Gα$_{i3}$. *D*, Gα$_{i3}$ binding to GST fusion proteins of GIRK1, normalized to G1–C3.

Gβγ binding sites (32). Fig. 1*C* shows that three fragments covering all of the proximal part of C terminus of GIRK1, G1–C1 through G1–C3, bound Gα$_{i3\text{-}GDP}$; G1–C3 showed the strongest binding (summarized in Fig. 1*D*). Interestingly, the whole C terminus (G1$_{183–501}$) bound Gα$_{i3}$ far weaker than G1–C3. It is possible that the complete C terminus is folded in such a way that the distal part beyond aa 380 (which was proposed to play a role of a "switch" that regulates the activation of the channel in protein kinase A-dependent manner (34–36)) impedes the binding of Gα$_i$ to the main C-terminal binding segments.

We also examined Gα$_{i3}$ binding to GIRK2 using GST-fused GIRK2 segments shown in Fig. 2*A* (sequence alignments of N termini and parts of the C termini of GIRK1 and GIRK2 are shown in Fig. 2*B*). The strongest binding of Gα$_{i3\text{-}GDP}$ was observed in the large segment G2–C2, aa 310–414, and in its smaller subdivision G2–C1–2 (aa 310–380) (Fig. 2*C*; summarized in Fig. 2*D*). This segment mostly overlaps G1–C3 of GIRK1 except the first 20 aa (Fig. 2*B*, *part b*). The first half of the N terminus did not bind Gα$_{i3}$, whereas the second half bound Gα$_{i3\text{-}GDP}$, although apparently somewhat weaker than G2–C2–1. The absence of Gα$_{i3}$ binding to G2–C1–2, which lacks 20 C-terminal aa compared with the homologous G1–C2 that binds Gα$_{i3}$ well, hints that this 20-aa stretch contains an important binding determinant for Gα$_{i3}$.

Incubation of *in vitro* synthesized Gα$_{i3}$ with GTPγS protected Gα$_{i3}$ from trypsin digestion, as expected for a GTPγS-bound Gα (37) (Fig. 3*A*). This result confirms GTPγS binding and the consequent change in Gα conformation and attests to functional integrity of *in vitro* synthesized Gα$_{i3}$ protein. Under mild non-ionic detergent conditions (0.05% Tween 20), the extents of binding of Gα$_{i3\text{-}GDP}$ and Gα$_{i3\text{-}GTP\gamma S}$ to the N terminus of GIRK1 were comparable (Ref. 14 and data not shown). However, under the standard conditions used in most experiments, with 0.5% CHAPS, the binding of Gα$_{i3\text{-}GTP\gamma S}$ was weaker than that of Gα$_{i3\text{-}GDP}$ (Fig. 3*C*). The same was observed with the C-terminal G1–C3 segment (Fig. 3, *B* and *C*). The summary in Fig. 3*C* shows that, in 0.5% CHAPS, the binding of Gα$_{i3\text{-}GTP\gamma S}$ to all Gα-binding fusion segments of GIRK1 and GIRK2 was only about a third of that of Gα$_{i3\text{-}GDP}$ (Fig. 3*C*).

The Gα$_{i3}$ binding segments identified by pull-down also bind Gβγ (32). To rule out the possibility that Gα$_{GDP}$ binds to GIRK indirectly, via Gβγ present in the reticulocyte lysate, we performed two types of control experiments. First, we verified that binding of Gα$_{i3}$ to different segments was not increased by the addition to the reaction mixture of various amounts of untreated reticulocyte lysate, suggesting that the binding of Gα$_{i3\text{-}GDP}$ to GIRK was not via an endogenous protein present in the lysate (data not shown). Second, addition of lysate containing *in vitro* synthesized Gβ$_{1γ2}$ did not increase the binding of Gα$_{i3\text{-}GDP}$ to G1$_{1–84}$ and G1–C1 (data not shown). Two additional facts argue against involvement of Gβγ in mediating Gα$_{i3}$ binding to GIRK: 1) the binding preference for Gβγ in the C terminus of GIRK1 (G1–C1 > G1–C2 > G1–C3; see Ref. 32) is opposite to that of Gα$_{i3}$ and 2) Gα$_{i1\text{-}GDP}$ does not bind to G1–C3 (see below), despite the very high affinity of binding of Gα$_{i1\text{-}GDP}$ to Gβγ (38). We conclude that, under our experimental conditions, Gα$_{i3}$ binds directly to GST-fused segments of GIRK1.

Preliminary screening of several Gα subunits indicated weak binding of Gα$_{i1\text{-}GDP}$ to fusion proteins of GIRK1. We thus focused on the comparison of Gα$_{i3}$ and Gα$_{i1}$. Functional integrity of Gα$_{i1}$ was verified by the trypsin digestion test (data not shown). For each GST fusion protein, the binding reaction was performed with equal volumes of reticulocyte lysate containing

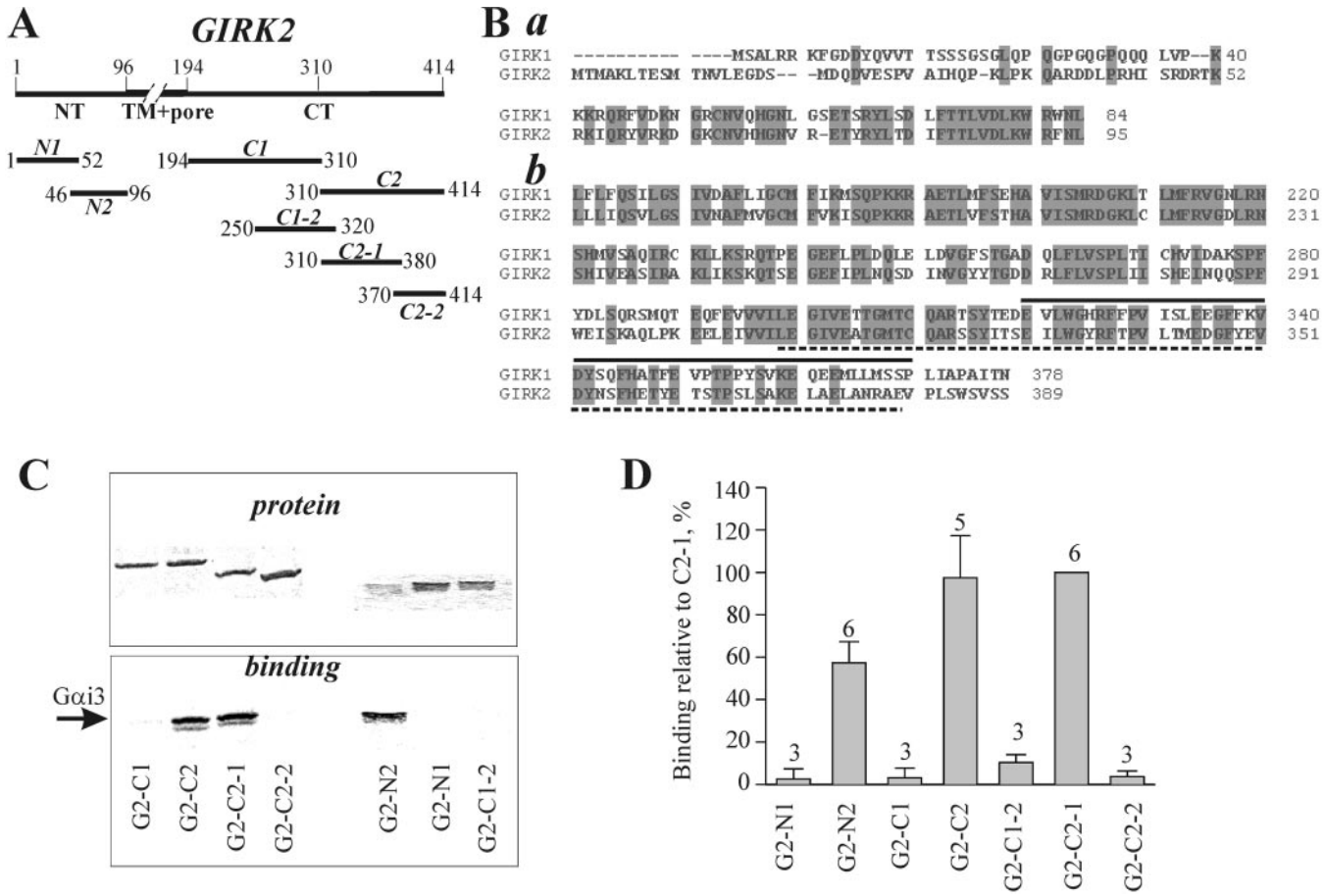

FIG. 2. **Binding of $G\alpha_{i3\text{-}GDP}$ to GST-fused fragments of GIRK2.** *A*, linear presentation of GIRK2 protein is shown at the *top*, and the GST fusion proteins used in this study are shown *below*. *B*, sequence alignment of N terminus (*a*) and part of C terminus (*b*) of GIRK1 and GIRK2. The segments G1–C3 and G2–C2–1 are denoted by *solid* and *dashed lines*, respectively, above GIRK1 and below GIRK2. *C*, binding of $G\alpha_{i3\text{-}GDP}$ to GST fusion proteins of GIRK2. *Upper panel* shows Coomassie Blue staining of eluted GST fusion proteins; the *lower panel* shows the autoradiogram of bound $G\alpha_{i3}$. *Left* and *right halves* show results from two separate gels. *D*, summary of binding of $G\alpha_{i3\text{-}GDP}$ to GIRK2 fusion proteins, normalized to G2–C2–1.

FIG. 3. **Differences in binding of $G\alpha_{i3\text{-}GDP}$ and $G\alpha_{i3\text{-}GTP\gamma S}$ to GST-fused fragments of GIRK1 and GIRK2.** *A*, trypsin digests GDP-, but not GTPγS-bound $G\alpha_{i3}$. *B*, comparison of binding of $G\alpha_{i3\text{-}GTP\gamma S}$ and $G\alpha_{i3\text{-}GDP}$ to G1–C3 (*lower panel*, *binding*). *Input* (*upper panel*) denotes the radioactive signal from a 5-μl sample of the reaction mixture (out of a total of 300 μl), taken before the addition of glutathione affinity beads. *C*, summary of binding of $G\alpha_{i3\text{-}GTP\gamma S}$ to GST fusion proteins of GIRK1 and GIRK2, presented as percent of $G\alpha_{i3\text{-}GDP}$ binding measured in the same experiments.

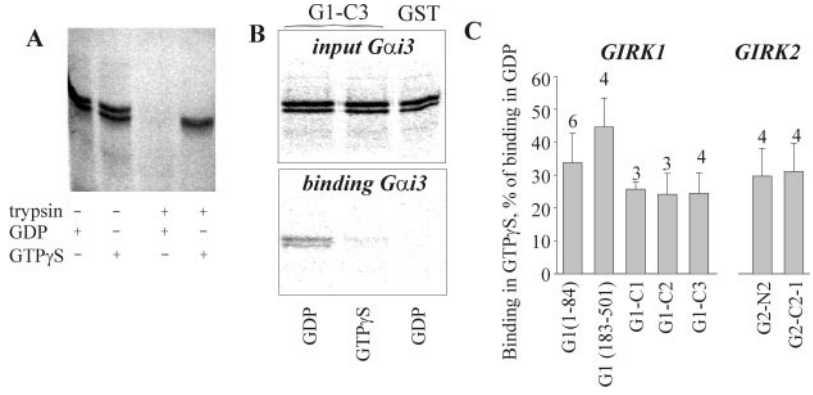

the labeled $G\alpha$ subunits, and the amount of bound $G\alpha$ was normalized to the amount of $G\alpha$ added to the reaction in the beginning ("input"). Figs. 4 (*A* and *B*) show examples of individual experiments, and Fig. 4*C* summarizes the results of all experiments with all GST fusion segments, showing the binding of $G\alpha_{i1}$ relative to $G\alpha_{i3}$. In all segments of GIRK1 tested, the binding of $G\alpha_{i1\text{-}GDP}$ was consistently weaker than that of $G\alpha_{i3\text{-}GDP}$ (Fig. 4, *A* and *C*), and the binding of $G\alpha_{i1\text{-}GTP\gamma S}$ was too weak to be reliably quantitated (data not shown). Some $G\alpha_{i1}$ binding was observed in the N terminus, confirming a previous finding (12), but it amounted only to about 20% of $G\alpha_{i3\text{-}GDP}$. G1–C3 did not bind $G\alpha_{i1\text{-}GDP}$ at all. In GIRK2, both $G\alpha_{i3}$-binding segments (G2–N2 and G2–C2–1) gave very weak signal with $G\alpha_{i1\text{-}GDP}$ (Fig. 4, *B* and *C*).

We utilized *Xenopus* oocytes to examine how coexpressed $G\alpha_{i3}$ and $G\alpha_{i1}$ affect the function of GIRK and to see whether their effect on various parameters of channel function correlate with the observed differences in their binding. To avoid promiscuous interactions caused by excessive expression of signaling proteins, which may obscure specificity (39), it is important to avoid overexpression and to titrate protein levels (which do not necessarily correlate with the amount of injected RNA). Titration of protein levels was especially important when comparing the effects of two homologous $G\alpha$ proteins, $G\alpha_{i3}$ and

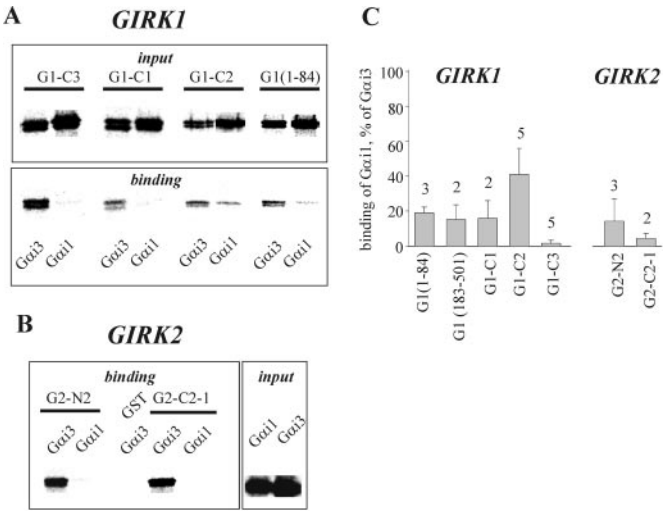

FIG. 4. **Gα_{i3} binds to GIRK subunits better than Gα_{i1}.** *A*, comparison of binding of G$\alpha_{i1\text{-}GDP}$ and G$\alpha_{i3\text{-}GDP}$ to GST-fused fragments of GIRK1. Results of several representative experiments are shown. The terms *input* and *binding* have the same meaning as in Fig. 2*C*. *B*, comparison of binding of Gα_{i1} and Gα_{i3} to GST-fused fragments of GIRK2. A representative experiment is shown. *C*, summary of experiments like those in *A* and *B* for G$\alpha_{i1\text{-}GDP}$ and G$\alpha_{i3\text{-}GDP}$. For each GST fusion protein, the binding of G$\alpha_{i1\text{-}GDP}$ was presented as percent of binding of G$\alpha_{i3\text{-}GDP}$, after correction for differences in inputs of Gα_{i1} and Gα_{i3}.

Gα_{i1}, to avoid a situation in which the weakly interacting Gα_{i1}, present at high levels, "mimics" the effects of the strongly interacting but poorly expressed Gα_{i3}.

The protein levels of Gα_{i3} and Gα_{i1} were measured upon injection of 1 ng of RNA/oocyte, an amount widely used in functional experiments (see below). The amounts of Gα were quantitated using Western blot methodology with a common Gα_i antibody. Because it is possible that the antibody does not bind with the same affinity to Gα_{i1} and Gα_{i3}, we performed a calibration procedure. [^{35}S]Met-labeled Gα_{i1} and Gα_{i3} were synthesized in reticulocyte lysate, run on gel, and transferred to a blot membrane. The radioactive signal from the membrane (Fig. 5*A*, "*PhosphorImager*") was compared for the two proteins and corrected for the number of methionines in each molecule, giving the relative molar amounts of each protein on the blot membrane (normalized to Gα_{i3}). The chemiluminescence signal obtained from Western blot of the same blot membrane (Fig. 5*A*) could then be calibrated to give a correction factor (equal to 1 if the antibody recognized the two proteins equally well), which can be used to correct the quantitative results from Western blots of Gα in any cell. Gα_{i1} and Gα_{i3} (1 ng of RNA) were expressed in oocytes, and signals from Western blots of membrane fractions (Fig. 5*B*) were quantitated and corrected. The results indicated similar levels of expression of the two Gα proteins, with a slight preference toward Gα_{i1} (~40%; Fig. 5*C*).

In most cases the choice of amounts of RNAs injected for functional experiments was based on titrations made in our previous works and designed to avoid excessive protein levels. Heterotetrameric GIRK1/2 channels were expressed either at a low level (density), 0.025–0.05 ng of RNA/oocyte of each GIRK subunit, or at a high density (1 ng of RNA/oocyte). The amounts of RNAs of Gα subunits were varied depending on the density of expressed channel (14). To activate GIRK, human m2 receptor (m2R) was expressed at 0.5 ng of RNA per oocyte, sufficient to activate all expressed GIRK channels (23). No coexpression of G$\beta\gamma$ is needed, because the oocytes usually have high levels of endogenous G$\beta\gamma$ sufficient for activation of all GIRK channels even when those are at high density (14).

Whole cell GIRK currents were studied in intact oocytes under two-electrode voltage clamp. Exchanging the external solution from a low K^+ (2 mM) ND96 solution to a high K^+ (24 mM) solution revealed the basal GIRK current, I_{basal}. Addition of 10 μM acetylcholine elicited the agonist-evoked current, I_{ACh} (Fig. 6*A*). When GIRK was expressed at low density (15–50 pg of RNA of each channel subunit per oocyte), coexpression of an excess of Gα_{i3} or Gα_{i1} (0.5 ng of RNA) reduced I_{basal} by about half (Fig. 6*B*, *part a*). I_{ACh} was not altered in Gα_{i1}-expressing cells but augmented in Gα_{i3}-expressing cells ($p < 0.01$, Fig. 6*B*, *part c*). The total GIRK current ($I_{total} = I_{basal} + I_{ACh}$) was not affected by the expression of either Gα_{i1} or Gα_{i3} (Fig. 6*B*, *part e*). The relatively modest effects of Gα_{i3} at low densities of GIRK can be attributed to the presence of sufficient amounts of endogenous G$\alpha_{i/o}$ that are able to sustain agonist-induced currents that are above basal agonist-independent activity, even without the coexpressed Gα_i (14).

When GIRK was expressed at high densities (1 ng of RNA/oocyte), expression of 0.5 ng of RNA of Gα_{i1} or Gα_{i3} did not affect I_{basal} and slightly enhanced I_{ACh} (data not shown). Expression of excess Gα_{i1} or Gα_{i3} (5 ng of RNA) greatly reduced I_{basal} and significantly enhanced I_{ACh} (Fig. 6*B*, *parts b* and *d*), as reported (14). However, I_{total} was reduced, especially by Gα_{i1} (Fig. 6*B*, *part f*). Gα_{i3} appeared to cause a stronger enhancement than Gα_{i1}, but the difference was not statistically significant. The strong reduction in I_{basal} and a decrease in I_{total} suggest a substantial scavenging of free G$\beta\gamma$, and much of the enhancement of I_{ACh} with both Gα proteins may reflect a greater available pool of G$\beta\gamma$ donors. Also, it is possible that excess of the "poor" interacting partner (Gα_{i1}) saturates the expressed channels, mimicking the preferred partner (Gα_{i3}) and masking the differences in efficiency of coupling with the channel. Therefore, we injected moderate amounts of RNA of Gα_{i1} or Gα_{i3}, 1 ng/oocyte. This caused only a slight ~20% reduction of I_{basal} (Fig. 5*B*, *part b*), whereas I_{ACh} was substantially increased: by 89 ± 14.6% by Gα_{i1}, and by 178 ± 18% by Gα_{i3} (Fig. 5*B*, *part d*; see examples in Fig. 5*A*). The enhancement by Gα_{i3} was significantly greater than by Gα_{i1} ($p < 0.01$). I_{total} was not changed by Gα_{i1} and slightly but significantly increased by Gα_{i3}. If the G_{i3} heterotrimer is superior to G_{i1} in forming a complex with GIRK, and if such complexes exist prior to activation of the GPCR by agonist, a faster kinetics of activation of I_{ACh} with Gα_{i3} may be expected (13, 40). Fig. 6*C* shows that this was indeed the case: coexpression of Gα_{i3} significantly ($p < 0.01$) accelerated the kinetics of activation of I_{ACh}, measured as time to 90% of peak I_{ACh} ($t_{90\%}$). Gα_{i1} also reduced the activation time ($p < 0.05$), but less than Gα_{i3}. Although finite speed of perfusion (about 1 s) imposed a lower limit on measurements of activation time in these experiments, the remarkable acceleration of activation by Gα_{i3} (from 8.8 ± 2.1 s in control to 1.8 ± 0.3 s in the presence of Gα_{i3}) cannot be an artifact of insufficiently fast wash in of the solution.

In intact cells, the increase in I_{ACh} may result from a larger pool of G$\alpha\beta\gamma$ available as donors of free G$\beta\gamma$, but also from an effect of Gα_i on GIRK gating (14). The relative contribution of these factors to Gα_i-induced increase in I_{ACh} cannot be explicitly estimated from whole cell recordings. In contrast, when GIRK is activated by purified G$\beta\gamma$ in excised membrane patches, activation is receptor-independent and bypasses the donor stage. Activation of GIRK by G$\beta\gamma$ in excised patches, relative to basal activity, is augmented by Gα_{i3} (a priming effect) (14). To inquire whether Gα_{i1} can prime GIRK for activation by G$\beta\gamma$ in excised patches, we injected the oocytes with amounts of RNAs of Gα_{i1} or Gα_{i3}, which were slightly greater than of GIRK (1 ng of each GIRK subunit and 2 ng of Gα, or 2 ng of GIRK and 3 ng of Gα). In most experiments m2R was not expressed. Typical records made 3–4 days after RNA injection

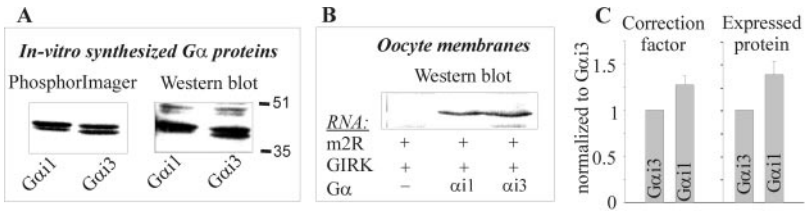

FIG. 5. **Estimating the levels of expression of $G\alpha_{i1}$ and $G\alpha_{i3}$ subunits after calibration of Western blot signals.** *A*, comparison of radioactive (PhosphorImager) and chemiluminescence (Western blot) signals from *in vitro* synthesized, [^{35}S]methionine-labeled Gα subunits. *B*, Western blot of total oocyte membrane fraction with the same antibodies is shown. All RNAs were 1 ng/oocyte except m2R, which was 0.5 ng/oocyte. *C*, relative amounts of expressed Gα measured from blots like that in *B* ($n = 3$; *right panel*), after correction using correction factors (*left panel*) for antibody signals measured from three experiments like that shown in *A*.

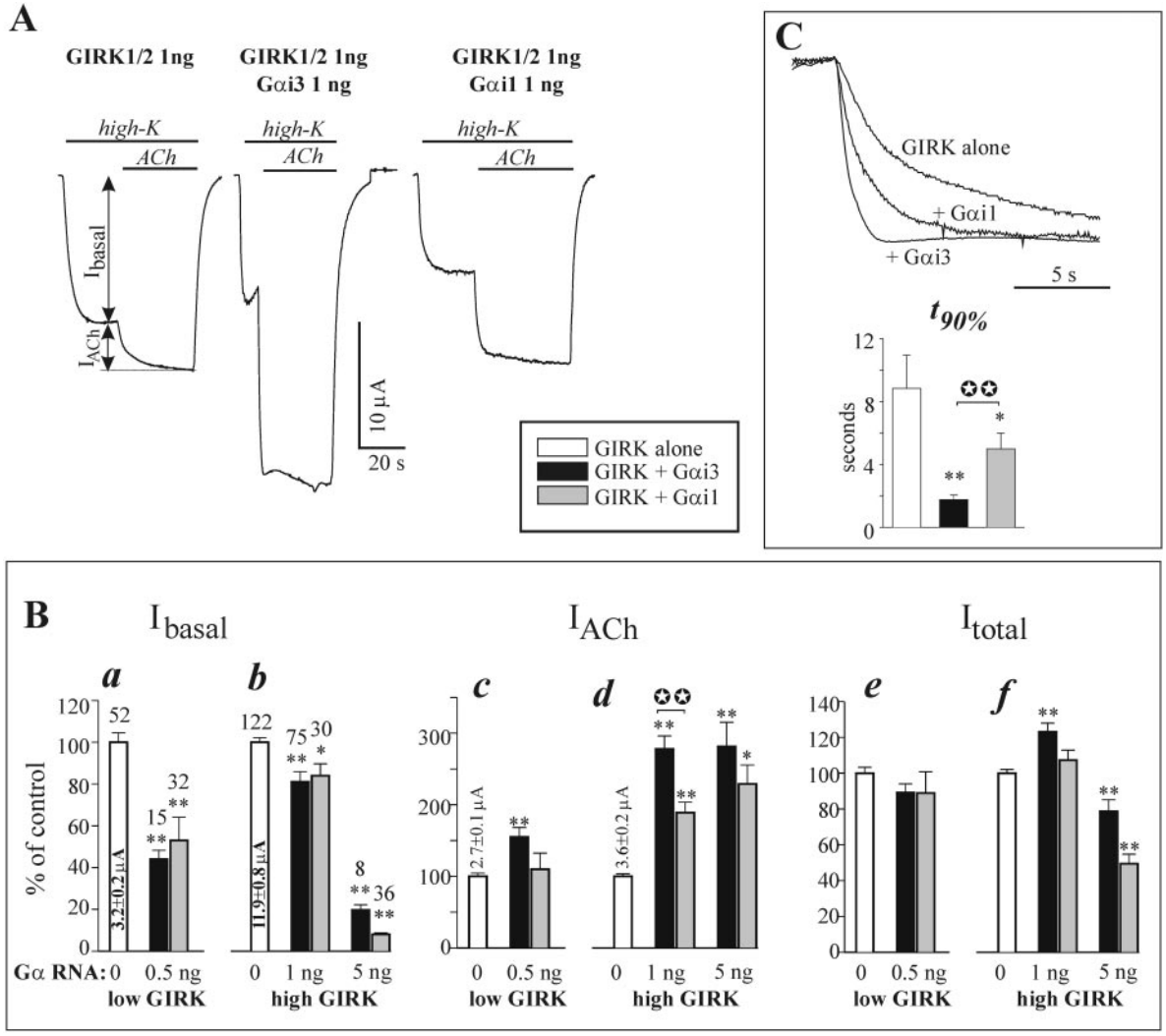

FIG. 6. **Effects of coexpression of $G\alpha_{i3}$ and $G\alpha_{i1}$ on whole-cell GIRK1/2 currents in *Xenopus* oocytes.** The code for *bar shading* for *panels B* and *C* is shown in the *inset* in the *middle* of the *figure*. *A*, representative current records in oocytes expressing the channel alone (*left*), with $G\alpha_{i3}$ (*center*), or with $G\alpha_{i1}$ (*right*). Each oocyte was injected with 1 ng of each RNA except m2R, which was 0.5 ng. *B*, summary of effects of $G\alpha_{i1}$ and $G\alpha_{i3}$ on amplitudes of basal, ACh-evoked, and total GIRK currents. I_{basal}, I_{ACh}, and I_{total} in each oocyte were normalized to the average current recorded in control group (*no Gα*) of the same oocyte batch, and averaged across all experiments (see Ref. 14). *C*, comparison of kinetics of activation of I_{ACh} in oocytes expressing different Gα proteins. The *upper panel* shows the first 14 s of I_{ACh} in the same oocytes shown in *A*. Currents were scaled to allow a direct comparison of speed of activation. The *lower panel* shows a summary of measurement of $t_{90\%}$ from 18–20 oocytes. *, $p < 0.05$; **, $p < 0.01$ compared with control (*no Gα*). *Filled circle* with *stars* indicates significant difference between $G\alpha_{i1}$ and $G\alpha_{i3}$ groups, $p < 0.01$.

are shown in Fig. 7*A*. On the average, levels of basal activity recorded in cell-attached (c.a.) configuration were reduced by each Gα compared with the control group where the channel was expressed alone (Fig. 7*B*, *part a*). The basal activity in these experiments corresponded to medium to high channel density (see Ref. 14).

After 1–2 min of c.a. recording, the patch was excised into a Na^+- and GTP-free, high K^+ bath solution that contained 2 mM MgATP (the latter is needed to sustain viable levels of phosphatidylinositol bisphosphate, necessary for proper GIRK function (41)). After an initial reduction, which was similar in all oocyte groups (not shown), the basal activity stabilized. 20 nM purified recombinant Gβγ was added 3 min after excision, and activation relative to basal activity in the same patch was measured. The results are presented as -fold activation relative to either basal c.a. activity (Fig. 7*B*, *part b*) or to basal activity

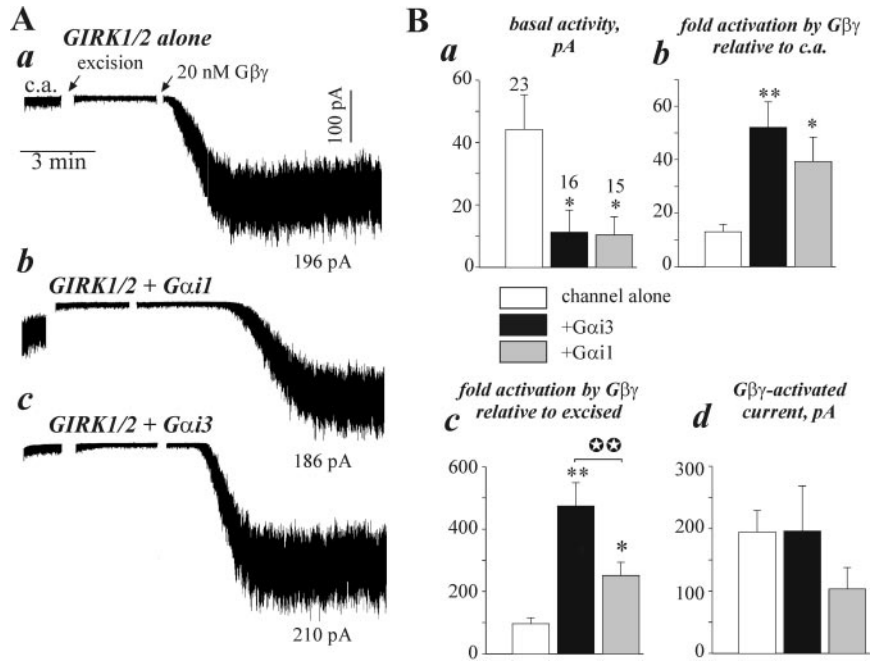

FIG. 7. **Coexpression of Gα$_{i3}$, but not Gα$_{i1}$, enhances Gβγ-evoked GIRK response in excised patches.** *A*, representative records from patches of three different oocytes expressing GIRK1/2 alone (*a*), with Gα$_{i1}$ (*b*), or Gα$_{i3}$ (*c*). *B*, parameters of GIRK activity recorded in patches: *a*, average basal activity in cell-attached patches, in pA; *b*, average extent of activation by 20 nM Gβγ relative to basal activity in the same patch in cell-attached configuration; *c*, extent of activation by 20 nM Gβγ relative to basal activity in the same patch measured after excision, during the last minute before the addition of Gβγ; *d*, total Gβγ-induced currents (in pA). *, $p < 0.05$; **, $p < 0.01$ compared with control (*no Gα*). *Filled circles* with *stars* indicates significant difference between Gα$_{i1}$ and Gα$_{i3}$ groups, $p < 0.01$.

in excised configuration (Fig. 7*B*, *part c*). Both types of analysis showed that both Gα$_{i3}$ and Gα$_{i1}$ enhanced Gβγ-induced activation, but Gα$_{i3}$ was more efficient, causing ~4-fold priming. Gα$_{i1}$ caused 2- to 3-fold priming. The absolute values of Gβγ-activated currents (which correspond to I_{total} in whole cell recordings) did not differ significantly in the three groups, although a certain tendency to decrease was observed in the presence of Gα$_{i1}$ (Fig. 7*B*, *part d*).

DISCUSSION

We have identified Gα$_{i3\text{-}GDP}$ binding sites in N- and C-terminal parts of the ubiquitous GIRK1 and the neuronal GIRK2 subunits and investigated the correlation between Gα$_i$ binding and the effect on channel function. Coexpression of Gα$_{i3}$ improved the speed and extent of agonist- and Gβγ-induced activation of GIRK. A homologous member of the Gα$_{i/o}$ family, Gα$_{i1}$, showed substantially weaker binding to GIRK than Gα$_{i3}$, and correspondingly served as a poorer donor of Gβγ and a weaker enhancer of Gβγ-dependent activation. Our results support the postulate (13, 14) that direct interactions of GDP-bound Gα$_i$ subunits (or Gαβγ heterotrimers) with GIRK regulate the biological effect of Gβγ and take part in determining signaling specificity. Active modulation of a Gβγ effector by Gα$_{GDP}$ (or Gα$_{GDP}$βγ) is a novel aspect of G protein signaling and warrants attention as a phenomenon that may exist in other G protein-coupled signaling pathways.

Gα$_{i3\text{-}GDP}$ Binds to Strategically Important Parts of GIRK—In addition to the previously identified N-terminal binding site in GIRK1 (12, 14), we found Gα$_{i3}$ binding sites in the N terminus of GIRK2 and in the C termini of both GIRK1 and GIRK2. The strongest binding was to the G1–C3 segment in GIRK1 (amino acids 320–370), and a homologous segment G2–C2–1 in GIRK2 (aa 310–380, correspond to aa 299–369 of GIRK1; see Fig. 3*B*). Gα$_{i1}$ binds much weaker than Gα$_{i3}$ to both GIRK subunits. The existence of multiple N- and C-terminal Gα$_i$-binding segments implies large Gα-interacting surfaces, which probably contribute to three-dimensional Gα$_i$ binding sites formed by one or more GIRK subunits.

According to the crystal structure of the cytosolic domain of GIRK1 (8), the Gα-binding segments lie at the surface of this domain and are exposed to cytosol, which makes them available for protein-protein interactions (see Fig. 1*A*). These segments harbor (or lie close to) aa residues crucial in the regulation of GIRK gating, for instance glutamate 304 in GIRK1 (315 in GIRK2) and some adjacent residues (42, 43). The sequence VDY (340–342 in GIRK1, 346–348 in GIRK2), which is homologous to IDY (aa 298–300) in KirBac1.1, and adjacent segments in other Kir channels, are sites of interaction with the N terminus, which play an important role in gating processes in Kir channels (9, 44). The N-terminal Gα binding sites in GIRK subunits contain, at the boundary with the first transmembrane α-helix, a stretch (aa 64–77 in GIRK1) highly conserved among all Kir channels (9). This segment in KirBac1.1 forms a "slide" helix linking the transmembrane, pore-forming part of the channel with the cytosolic domain; it has been proposed to play a key role in Kir gating by linking movements of the cytosolic domain and of transmembrane helixes M1 and M2 (9). Hence, the N- and C-terminal segments of GIRK that interact with Gα overlap, or are located close to, parts of channel molecule that are crucially involved in channel gating.

The binding sites for Gα$_{i3}$ are also spatially close to, and may partially overlap, the Gβγ binding sites found in the N and C termini (12, 32, 45, 46). This implies a complex pattern of interaction between G protein subunits and the channel, which may involve elements of competition and/or synergistic interactions. However, because the continued presence of coexpressed Gα$_{i3\text{-}GDP}$ does not impair (actually enhances) activation by added Gβγ in excised patches, competition between Gα$_{GDP}$ and Gβγ for binding to GIRK under physiological conditions appears unlikely.

Gα$_i$ as an Anchor and Donor of Gβγ—Anchoring of Gβγ (within a Gαβγ heterotrimer attached to the channel) and donating it upon addition of agonist is the most acknowledged potential function of Gα. Our working hypothesis, based on suggestions of Lily Jan and collaborators (12, 13) and later our own (14), is that physical interaction between Gα$_i$ and GIRK allows fast coupling between the GPCR and GIRK. It enables the formation of a signaling complex that includes Gα, Gβγ, and the effector and enhances signaling specificity. Here, we utilized the differences in Gα$_{i1}$ and Gα$_{i3}$ binding to GIRK1 and GIRK2 to further explore this hypothesis in *Xenopus* oocytes. These cells are uniquely suited for quantitative titration of protein levels by exactly varying the amounts of injected RNA

over a wide range. Here and previously (14), levels of expressed proteins have been also assessed by direct immunochemical measurements. Uncertainties introduced by possible differences in GPCR-Gα coupling were avoided by using m2R, which couples equally well to all members of $G\alpha_{i/o}$ family (47).

Mass action law dictates that, for similar expression levels of two $G\alpha_i$ species, more GIRK-G$\alpha\beta\gamma$ complexes will be formed with Gα that binds GIRK with higher affinity, as long as the expression level of Gα is non-saturating. The existence of such a complex will ensure faster activation by agonist than in the case when G$\beta\gamma$ diffuses from a non-anchored heterotrimer (30). Therefore, kinetics of activation provide reliable information on the efficiency of Gα-GIRK coupling (23, 48). Since I_{ACh} shows desensitization (reviewed in Ref. 5), faster activation should also result in a greater agonist response amplitude (49). However, the kinetic parameter is more informative, because the difference in amplitudes of I_{ACh} may also stem from the less well understood phenomenon of priming (see below) or from an increase in surface expression of GIRK caused by coexpression of $G\alpha_{i3}$ (14). We found both faster kinetics of activation and larger I_{ACh} with coexpressed $G\alpha_{i3}$ than with $G\alpha_{i1}$, supporting the hypothesis described above. The functional inferiority of $G\alpha_{i1}$ was seen at all doses of Gα tested. However, it was most prominent at moderate expression levels, and became less pronounced at high levels of $G\alpha_{i1}$. Such "promiscuous" coupling between poorly interacting proteins is common in heterologous expression systems upon overexpression of one of the components (39). This is in agreement with mass action law: when the concentration of $G\alpha_{i1}$ becomes saturating (presumably in great excess over GIRK), it should be able to cause the same maximal effect as $G\alpha_{i3}$ if the only difference between them is the affinity of interaction with GIRK. However, when expressed in excess, both $G\alpha_{i1}$ and $G\alpha_{i3}$ also act as general scavengers of G$\beta\gamma$, forming G$\alpha\beta\gamma$ heterotrimers not complexed with GIRK and reducing I_{total} (14). If less $G\alpha_{i1}$ is complexed with GIRK compared with $G\alpha_{i3}$, more $G\alpha_{i1}$ is available for general G$\beta\gamma$ scavenging. Our results support this notion: although $G\alpha_{i1}$ accelerates the activation and increases I_{ACh} at moderate and high expression levels, it never reaches the efficiency attained by $G\alpha_{i3}$ and causes a greater reduction in I_{total} than $G\alpha_{i3}$ at 5 ng of RNA/oocyte (Fig. 6*B*). In all, our results suggest that $G\alpha_{i1}$ is less efficient than $G\alpha_{i3}$ as a G$\beta\gamma$ donor for GIRK under most conditions.

The strength of Gα-GIRK interaction is not the only factor that determines the identity of $G\alpha_{i/o}$ that couples a GPCR to GIRK in native cells. Additional factors include coupling specificity at the GPCR-Gα interface (21) and Gα availability. Theoretically, a cell with excess $G\alpha_{i1}$ may preferentially use it for agonist signaling to GIRK. Yet, published data imply a preferential use of $G\alpha_{i3}$ (or $G\alpha_{i2}$) over $G\alpha_{i1}$ and $G\alpha_o$ to activate GIRK. An antibody- and antisense-based study suggested that somatostatin-induced GIRK current in AtT-20 cells critically depends only on $G\alpha_{i3}$, whereas in locus coeruleus neurons it is mediated by $G\alpha_{i2}$ and not by $G\alpha_{i1}$, $G\alpha_{i3}$, or $G\alpha_o$ (50). Notably, all $G\alpha_{i/o}$ subunits are present in the brain (51). In the atrium, despite the abundance of $G\alpha_o$ (52, 53), only $G\alpha_{i2}$ and $G\alpha_{i3}$, but not $G\alpha_o$ mediate the m2R-mediated GIRK current $I_{K(ACh)}$, as shown by targeted inactivation and re-expression of Gα subunits (54–56). Importantly, m2R does not prefer $G\alpha_{i2}$ or $G\alpha_{i3}$ over $G\alpha_o$, because it specifically uses $G\alpha_o$ to inhibit ventricular Ca^{2+} channels (55). Unfortunately, the role of $G\alpha_{i1}$ has not been specifically examined in these works, and its abundance in the heart is controversial (51, 53). A correlation between relative abundance of $G\alpha_{i2}$ or $G\alpha_{i3}$ and their use as the main donors of G$\beta\gamma$ cannot be ruled out at present.

Our results show that, in the zwitterionic detergent CHAPS, binding of $G\alpha_{i3\text{-}GTP\gamma S}$ to GIRK is significantly weaker than of $G\alpha_{i3\text{-}GDP}$. Stronger binding of $G\alpha_{i1\text{-}GDP}$ than $G\alpha_{i1\text{-}GTP}\gamma S$ to the N terminus of GIRK1 has also been reported (12). However, under mild non-ionic detergent conditions (0.05% Tween 20) the binding of $G\alpha_{i3}$ to N terminus of GIRK1 was not reduced by GTPγS (14). Even if measurements of binding in CHAPS accurately reflect the changes in Gα binding that take place *in vivo*, our results indicate that $G\alpha_{i\text{-}GTP}$ remains attached to the channel following the GPCR-catalyzed exchange of GDP to GTP. When GTP is hydrolyzed, fast recapture of G$\beta\gamma$ by closely positioned Gα would ensure fast deactivation upon washout of agonist. Indeed, for fast-dissociating agonist-receptor complexes, macroscopic deactivation is limited only by the speed of hydrolysis of GTP but not G$\beta\gamma$ dissociation form GIRK (57). The role of GPCR and of RGS proteins and the mode of their interaction with the G protein within such a multiprotein complex, remain to be elucidated.

$G\alpha_i$ as a Regulator of GIRK Gating and Function—Experiments in excised patches provide the opportunity to examine whether Gα affects the function of the channel in separation from the donor function. Added G$\beta\gamma$ (not G$\beta\gamma$ released from an endogenous G$\alpha\beta\gamma$ "donor" pool as in whole cell experiments) activates GIRK channels in the absence of coexpressed Gα. Coexpression of $G\alpha_{i3}$ not only reduces I_{basal} but also enhances activation of GIRK by G$\beta\gamma$, thus $G\alpha_{i3}$ serves as a primer for G$\beta\gamma$ effect (14). We proposed that this priming effect and part of the reduction in I_{basal} are the consequences of a direct interaction of $G\alpha_{i3}$ with the channel; we also envisaged a link between the two effects (14). The patch clamp experiments presented here showed that the extent of priming correlated with binding of $G\alpha_{i1}$ and $G\alpha_{i3}$. $G\alpha_{i3}$ enhanced GIRK activation caused by G$\beta\gamma$ in the absence of agonist or GPCR, and under the conditions of little general scavenging of G$\beta\gamma$ (as witnessed by the preservation of the amplitude of total G$\beta\gamma$-activated current). The weaker priming by $G\alpha_{i1}$ supports the view that this phenomenon depends on direct interaction between Gα and GIRK. Because the patches were excised into a GTP-free solution, it is most probable that the priming effect is caused by $G\alpha_{GDP}$ or G$\alpha\beta\gamma$ rather than $G\alpha_{GTP}$. On the other hand, $G\alpha_{i1}$ and $G\alpha_{i3}$ caused a similar reduction in I_{basal} (both in patches and in whole cells). This weakens the possibility of a direct inhibitory effect of $G\alpha_i$ on basal activity. However, because the latter appears to be mostly G$\beta\gamma$-dependent (14, 58), a direct scavenging of G$\beta\gamma$ may play a major role in the reduction of I_{basal} by Gα, masking a minor contribution of a direct effect of Gα. At present we do not understand the mechanism of the priming effect of $G\alpha_{GDP}$ and its linkage to the reduction in the basal activity. A possible scenario is one in which the channel possesses two types of G$\beta\gamma$ binding sites, one underlying the basal activity (high affinity site) and another, low affinity site responsible for agonist-evoked activity (46, 59). Gα, by forming a triple complex with G$\beta\gamma$ and the channel, prevents channel activation via the high affinity site, reducing I_{basal}, but changes the conformation of GIRK to enhance activation via the low affinity site once free G$\beta\gamma$ becomes available. Variants of this model may explain the known facts related to basal and evoked activities of GIRK, but a more specific formulation will require further experimentation.

Acknowledgment—We thank R. Barzilai for expert technical assistance.

REFERENCES

1. Clapham, D. E., and Neer, E. J. (1997) *Annu. Rev. Pharmacol. Toxicol.* **37,** 167–203
2. Stanfield, P. R., Nakajima, S., and Nakajima, Y. (2003) *Rev. Physiol. Biochem. Pharmacol.* **145,** 47–179
3. Wickman, K., Nemec, J., Gendler, S. J., and Clapham, D. E. (1998) *Neuron* **20,** 103–114

4. Dobrev, D., Graf, E., Wettwer, E., Himmel, H. M., Hala, O., Doerfel, C., Christ, T., Schuler, S., and Ravens, U. (2001) *Circulation* **104,** 2551–2557
5. Dascal, N. (1997) *Cell. Signal.* **9,** 551–573
6. Ikeda, K., Kobayashi, T., Kumanishi, T., Yano, R., Sora, I., and Niki, H. (2002) *Neurosci. Res.* **44,** 121–131
7. Mitrovic, I., Margeta-Mitrovic, M., Bader, S., Stoffel, M., Jan, L. Y., and Basbaum, A. I. (2003) *Proc. Natl. Acad. Sci. U. S. A.* **100,** 271–276
8. Nishida, M., and MacKinnon, R. (2002) *Cell* **111,** 957–965
9. Kuo, A., Gulbis, J. M., Antcliff, J. F., Rahman, T., Lowe, E. D., Zimmer, J., Cuthbertson, J., Ashcroft, F. M., Ezaki, T., and Doyle, D. A. (2003) *Science* **300,** 1922–1926
10. Wickman, K., and Clapham, D. E. (1995) *Physiol. Rev.* **75,** 865–885
11. Bichet, D., Haass, F. A., and Jan, L. Y. (2003) *Nat. Rev. Neurosci.* **4,** 957–967
12. Huang, C. L., Slesinger, P. A., Casey, P. J., Jan, Y. N., and Jan, L. Y. (1995) *Neuron* **15,** 1133–1143
13. Slesinger, P. A., Reuveny, E., Jan, Y. N., and Jan, L. Y. (1995) *Neuron* **15,** 1145–1156
14. Peleg, S., Varon, D., Ivanina, T., Dessauer, C. W., and Dascal, N. (2002) *Neuron* **33,** 87–99
15. Dascal, N. (2001) *Trends Endocrinol. Metab.* **12,** 391–398
16. Wickman, K. D., Iniguez-Lluhl, J. A., Davenport, P. A., Taussig, R., Krapivinsky, G. B., Linder, M. E., Gilman, A. G., and Clapham, D. E. (1994) *Nature* **368,** 255–257
17. Lei, Q., Jones, M. B., Talley, E. M., Schrier, A. D., McIntire, W. E., Garrison, J. C., and Bayliss, D. A. (2000) *Proc. Natl. Acad. Sci. U. S. A.* **97,** 9771–9776
18. Witherow, D. S., Wang, Q., Levay, K., Cabrera, J. L., Chen, J., Willars, G. B., and Slepak, V. Z. (2000) *J. Biol. Chem.* **275,** 24872–24880
19. Zhang, J. H., and Simonds, W. F. (2000) *J. Neurosci.* (*Online*) **20,** RC59
20. Leaney, J. L., Milligan, G., and Tinker, A. (2000) *J. Biol. Chem.* **275,** 921–929
21. Leaney, J. L., and Tinker, A. (2000) *Proc. Natl. Acad. Sci. U. S. A.* **97,** 5651–5656
22. Jeong, S. W., and Ikeda, S. R. (1998) *Neuron* **21,** 1201–1212
23. Vorobiov, D., Bera, A. K., Keren-Raifman, T., Barzilai, R., and Dascal, N. (2000) *J. Biol. Chem.* **275,** 4166–4170
24. Lim, N. F., Dascal, N., Labarca, C., Davidson, N., and Lester, H. A. (1995) *J. Gen. Physiol.* **105,** 421–439
25. Sorota, S., Rybina, I., Yamamoto, A., and Du, X. Y. (1999) *J. Physiol.* (*Lond.*) **514,** 413–423
26. Wellner-Kienitz, M. C., Bender, K., and Pott, L. (2001) *J. Biol. Chem.* **276,** 37347–37354
27. Sharon, D., Vorobiov, D., and Dascal, N. (1997) *J. Gen. Physiol.* **109,** 477–490
28. Kobrinsky, E., Mirshahi, T., Zhang, H., Jin, T., and Logothetis, D. E. (2000) *Nat. Cell Biol.* **2,** 507–514
29. Robillard, L., Ethier, N., Lachance, M., and Hebert, T. E. (2000) *Cell. Signal.* **12,** 673–682
30. Hille, B. (1994) *Trends Neurosci.* **17,** 531–536
31. Cohen, N. A., Sha, Q., Makhina, E. N., Lopatin, A. N., Linder, M. E., Snyder, S. H., and Nichols, C. G. (1996) *J. Biol. Chem.* **271,** 32301–32305
32. Ivanina, T., Rishal, I., Varon, D., Mullner, C., Frohnwieser-Steinecke, B., Schreibmayer, W., Dessauer, C. W., and Dascal, N. (2003) *J. Biol. Chem.* **278,** 29174–29183
33. Zamponi, G. W., Bourinet, E., Nelson, D., Nargeot, J., and Snutch, T. P. (1997) *Nature* **385,** 442–446
34. Medina, I., Krapivinsky, G., Arnold, S., Kovoor, P., Krapivinsky, L., and Clapham, D. E. (2000) *J. Biol. Chem.* **275,** 29709–29716
35. Mullner, C., Vorobiov, D., Bera, A. K., Uezono, Y., Yakubovich, D., Frohnwieser, B., Dascal, N., and Schreibmayer, W. (2000) *J. Gen. Physiol.* **115,** 627–633
36. Mullner, C., Yakubovich, D., Dessauer, C. W., Platzer, D., and Schreibmayer, W. (2003) *Biophys. J.* **84,** 1399–1409
37. Fung, B. K., and Nash, C. R. (1983) *J. Biol. Chem.* **258,** 10503–10510
38. Sarvazyan, N. A., Lim, W. K., and Neubig, R. R. (2002) *Biochemistry* **41,** 12858–12867
39. Chidiac, P. (1998) *Biochem. Pharmacol.* **55,** 549–556
40. Hille, B. (1992) *Neuron* **9,** 187–195
41. Logothetis, D. E., and Zhang, H. (1999) *J. Physiol.* (*Lond.*) **520,** 630
42. Chen, L., Kawano, T., Bajic, S., Kaziro, Y., Itoh, H., Art, J. J., Nakajima, Y., and Nakajima, S. (2002) *Proc. Natl. Acad. Sci. U. S. A.* **99,** 8430–8435
43. Guo, Y., Waldron, G. J., and Murrell-Lagnado, R. D. (2002) *J. Biol. Chem.* **277,** 48289–48294
44. Flagg, T. P., Yoo, D., Sciortino, C. M., Tate, M., Romero, M. F., and Welling, P. A. (2002) *J. Physiol.* (*Lond.*) **544,** 351–362
45. Kunkel, M. T., and Peralta, E. G. (1995) *Cell* **83,** 443–449
46. He, C., Yang, X., Zhang, H., Mirshahi, T., Jin, T., Huang, A., and Logothetis, D. E. (2002) *J. Biol. Chem.* **277,** 6088–6096
47. Migeon, J. C., Thomas, S. L., and Nathanson, N. M. (1995) *J. Biol. Chem.* **270,** 16070–16074
48. Benians, A., Leaney, J. L., Milligan, G., and Tinker, A. (2003) *J. Biol. Chem.* **278,** 10851–10858
49. Hille, B. (2002) *Ion Channels of Excitable Membranes*, Sinauer, Sunderland
50. Takano, K., Yasufuku-Takano, J., Kozasa, T., Nakajima, S., and Nakajima, Y. (1997) *J. Physiol.* (*Lond.*) **502,** 559–567
51. Kanaho, Y., Katada, T., Hoyle, K., Crooke, S. T., and Stadel, J. M. (1989) *Cell. Signal.* **1,** 553–560
52. Kawai, Y., and Arinze, I. J. (1996) *J. Mol. Cell Cardiol.* **28,** 1555–1564
53. Luetje, C., Tietje, K., Christian, J., and Nathanson, N. (1988) *J. Biol. Chem.* **263,** 13357–13365
54. Sowell, M. O., Ye, C., Ricupero, D. A., Hansen, S., Quinn, S. J., Vassilev, P. M., and Mortensen, R. M. (1997) *Proc. Natl. Acad. Sci. U. S. A.* **94,** 7921–7926
55. Valenzuela, D., Han, X., Mende, U., Fankhauser, C., Mashimo, H., Huang, P., Pfeffer, J., Neer, E. J., and Fishman, M. C. (1997) *Proc. Natl. Acad. Sci. U. S. A.* **94,** 1727–1732
56. Gilchrist, A., Bünemann, M., Li, A., Hosey, M. M., and Hamm, H. E. (1999) *J. Biol. Chem.* **274,** 6610–6616
57. Doupnik, C. A., Davidson, N., Lester, H. A., and Kofuji, P. (1997) *Proc. Natl. Acad. Sci. U. S. A.* **94,** 10461–10466
58. Petit-Jacques, J., Sui, J. L., and Logothetis, D. E. (1999) *J. Gen. Physiol.* **114,** 673–684
59. He, C., Zhang, H., Mirshahi, T., and Logothetis, D. E. (1999) *J. Biol. Chem.* **274,** 12517–12524
60. Doyle, D. A., Morais Cabral, J., Pfuetzner, R. A., Kuo, A., Gulbis, J. M., Cohen, S. L., Chait, B. T., and MacKinnon, R. (1998) *Science* **280,** 69–77